

Intercellular contact is sufficient to drive fibroblast-to-myofibroblast transitions

Vasuretha Chandar¹, Benjamin M. Goykadosh¹, Harikrishnan Parameswaran^{1*}

¹Department of Bioengineering, Northeastern University, Boston, MA, USA

*Corresponding Author Email: h.parameswaran@northeastern.edu

Abstract

Fibroblast cells play a key role in maintaining the extracellular matrix. During wound healing, fibroblasts differentiate into highly contractile myofibroblasts, which secrete extracellular matrix proteins like collagen to facilitate tissue repair. Under normal conditions, myofibroblasts undergo programmed cell death after healing to prevent excessive scar formation. However, in diseases like fibrosis, the myofibroblasts remain active even after the wound is closed, resulting in excessive collagen buildup and a stiff, fibrotic matrix. The reasons for the persistence of myofibroblasts in fibrosis are not well understood. Here we show the existence of a mechanism where direct physical contact between a fibroblast and a myofibroblast is sufficient for fibroblasts to transition into myofibroblasts. We show that fibroblast-myofibroblast transition can occur even in the absence of known biochemical cues such as growth factor activation or mechanical cues from a stiff, fibrotic matrix. Further, we show that contact-based fibroblast-myofibroblast activation can be blocked by Gαq/11/14 inhibitor FR9003591, which inhibits the formation of myofibroblasts. These findings offer new insights into the persistence of fibrosis despite therapeutic interventions and suggest a potential strategy to target fibroblast-to-myofibroblast transition in fibrosis.

Significance Statement

This study reveals novel mechanisms in fibroblast-to-myofibroblast transition (FMT) during fibrosis, challenging traditional views. It demonstrates that direct cell-cell contact between fibroblasts and myofibroblasts can induce FMT, independent of biochemical or mechanical cues. The GqGPCR signaling pathway is identified as a mediator of contact-induced FMT, presenting a new target for anti-fibrotic therapies. Increased cytoskeletal tension in fibroblasts is shown to precede and drive FMT, suggesting potential mechano-therapeutic approaches. These

findings expand our understanding of fibrosis beyond chemical and mechanical cues, highlighting the role of cell-cell interactions and intercellular mechanical forces. By addressing a critical gap in knowledge regarding myofibroblast persistence, this research opens new avenues for therapeutic intervention and contributes to a more comprehensive approach to fibrosis treatment.

Introduction

Idiopathic Pulmonary Fibrosis (IPF) is a chronic, progressive interstitial lung disease of unknown etiology ^{1,2}. Despite the lack of a clear cause, several risk factors have been identified, including aging and air pollution, which can trigger injury to lung tissues ^{3,4}. At the site of injury, one of the key cellular processes is the transformation of resident fibroblasts into highly contractile myofibroblasts ⁵. These specialized cells, characterized by α -smooth muscle actin (α -SMA) expression, play a crucial role in wound contraction and tissue remodeling at the site of injury by depositing extracellular matrix components, particularly collagen, to facilitate tissue repair ⁶⁻¹². In normal wound healing, once tissue integrity is restored, myofibroblasts are typically deactivated and cleared from the site ^{13,14}. However, in IPF, this process becomes dysregulated, leading to persistent activation and accumulation of myofibroblasts ^{14,15}. This results in excessive collagen deposition, causing scarring, stiffening, and fibrosis of the lung tissue. The stiffening of the lung severely impairs the ability of the lungs to facilitate oxygen and carbon dioxide exchange, leading to organ dysfunction - contributing to the progressive nature of the disease, leading to hypoxemia, loss of quality of life, and ultimately death ¹⁶.

Therefore, the persistence of the myofibroblast phenotype plays a crucial role in the progression of IPF. Current therapeutic strategies aim to prevent or reverse myofibroblast activation through two main approaches. The first involves targeting biochemical pathways and growth factors such as the WNT/ β -catenin, PDGF, TNF- α among others¹⁷. Existing drugs (ex: Nintedanib, Pirfenidone) inhibit growth factors and cytokines which prevent the release of inflammatory signals that trigger the transition of fibroblasts to myofibroblasts ^{18,19}. The second approach recognizes the mechanosensitive nature of these cells and focuses on matrix remodeling.

Myofibroblasts sense and respond to the stiff matrix environment created by excessive collagen deposition, reinforcing a perpetual positive feedback loop. To counteract this cycle, ongoing in vitro and in vivo studies are investigating matrix remodeling as a potential therapeutic approach²⁰⁻²². These studies utilize collagen-degrading enzymes, such as matrix metalloproteinases (MMPs), to soften the matrix and potentially halt the positive feedback loop, aiming to reverse the myofibroblast phenotype²³⁻²⁵. However, despite these interventions and approaches, a successful method to reverse the transition has not yet been established, and diseases like IPF continue to progress and pose significant challenges in finding a cure to alleviate the disease²⁶⁻²⁹.

The purpose of this work is to investigate alternative mechanisms responsible for the persistence of myofibroblasts in fibrotic conditions. While traditional understanding has focused on chemical signals and stiff matrix mechanical cues as primary drivers of fibrosis, these factors alone do not fully explain the sustained presence of myofibroblasts. This prompts the exploration of additional, independent pathways that might contribute to the progression and maintenance of fibrotic tissue. By examining the persistence of myofibroblasts in environments where known chemical and mechanical signals are absent or altered, this study aims to uncover novel mechanisms driving fibrosis. Understanding these alternative mechanisms is crucial for developing more comprehensive therapeutic strategies to address fibrotic diseases, as targeting multiple pathways simultaneously may prove more effective in halting or reversing the fibrotic process.

Results

1. Fibroblasts can transition to myofibroblasts independent of chemical and mechanical signals from the extra cellular matrix

Prior and ongoing research has aimed to address biochemical and mechanical pathways in fibrosis using growth factors, cytokine inhibitors, or collagen-degrading enzymes to reverse myofibroblast activation and reduce ECM rigidity. However, these methods have not conclusively reversed fibrosis, and conditions like idiopathic pulmonary

fibrosis (IPF) continue to deteriorate^{30,31}. This implies the presence of additional mechanisms beyond the known chemical and mechanical signals that drive the progression of fibrosis.

To investigate whether fibroblasts can transition to myofibroblasts without external chemical or mechanical cues, we utilized the property of mechanical memory of fibroblast cells, wherein extended exposure of fibroblasts to a stiff substrate preserved its pro-fibrotic behavior even after switching to healthy soft matrix conditions, such as expression of f-actin and α -SMA in their stress fibers^{32,33}. We generated two distinct cell populations: a pure fibroblast population that do not express α -SMA in stress fibers by prolonged culture on a 300Pa soft substrate. To clearly identify fibroblasts in a co-culture with myofibroblasts, we labelled them with a fluorescent td-tomato reporter. A pure myofibroblast population was generated by culturing fibroblasts on tissue culture plastic ($E \geq 100\text{kPa}$), for a period of 4 weeks. These cells were unlabeled but strongly expressed α -SMA in their stress fibers. The cells were then seeded (10^5 cells/cm²) on a 300Pa soft substrate (NuSil, PDMS) for 72 hours under standard cell culture conditions. Importantly, during this culture period, no external mechanical (e.g., increased substrate stiffness) or chemical stimuli (e.g., TGF β) were introduced to facilitate any transition. Cells were stained for filamentous actin (F-actin) and alpha-smooth muscle actin (α -SMA) to assess their phenotypic characteristics and nuclear spread area of cells were calculated³⁴. Our findings revealed a transition of fibroblasts to myofibroblasts after 72h, wherein cells that initially exhibited fibroblast characteristics, subsequently showed sequestration of α -SMA in their stress fibers (Fig 1A), a characteristic of myofibroblast phenotype. This result indicates that when fibroblasts are co-cultured (1:1) with myofibroblasts on a 300Pa substrate, they can undergo a phenotypic shift to myofibroblasts despite not being on a stiff substrate. Notably, this transition occurs in the absence of external chemical or mechanical stimuli, suggesting that cell-cell interactions within the co-culture environment may be responsible for driving this phenotypic change.

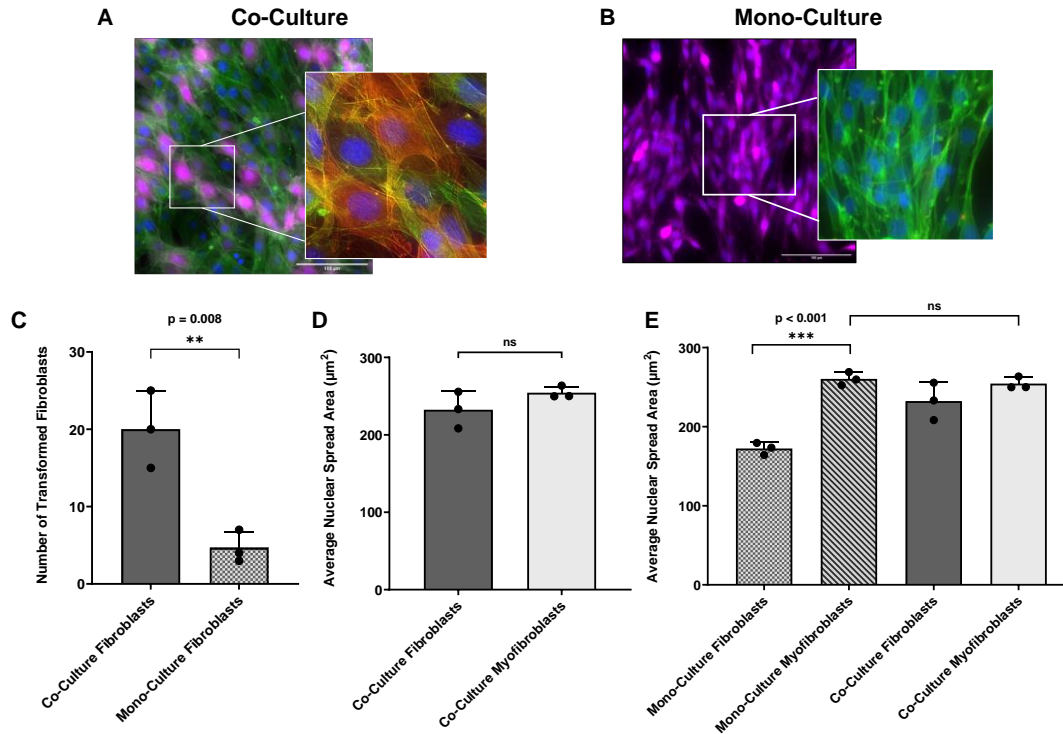


Fig 1: Fibroblasts when co-cultured with myofibroblasts undergo a phenotypic shift to myofibroblasts in the absence of external chemical or stiff matrix mechanical cues. Cells were stained for myofibroblast markers f-actin (green) and α -SMA (red) and nuclear stain DAPI (blue) after 3 days in culture. **(A)** Fibroblasts (magenta) in co-culture with myofibroblasts showed sequestration of α -SMA in their stress fibers when cultured on a 0.3kPa soft substrate, as in the inset (indicated by reddish yellow stress fibers). **(B)** Fibroblasts in mono-culture on 0.3kPa soft substrate retained their phenotype when not in contact with myofibroblasts. **(C)** At least 20% of the fibroblasts transformed into myofibroblasts ($p = 0.003$, unpaired t-test). **(D)** There is no significant difference in the nuclear spread area of fibroblasts in a co-culture compared to myofibroblasts in the co-culture (unpaired t-test, $n=3$). **(E)** There is no significant difference in the nuclear spread area of fibroblasts and myofibroblasts in the co-culture when compared to that of myofibroblasts in a mono-culture (One-way ANOVA, $n=3$).

2. Cell-cell contacts are required for fibroblast-to-myofibroblast transition in the absence of external cues

To investigate the primary mechanism underlying the transition of fibroblasts to myofibroblasts, specifically in the absence of external cues, an experimental system using a physical barrier was designed. Here, the fibroblasts and

myfibroblasts were separated (~ 1.5 mm) by a physical barrier which prevented direct cell-cell contact between the two cell phenotypes (Fig 2A) but it allowed for the diffusion of any intrinsic chemical signals (Fig 2B, 2C). Fibroblasts and myfibroblasts were seeded on either side of the physical barrier on the 300Pa soft substrate. The cells were cultured under standard cell culture conditions for 72 hours. Cells were then stained for f-actin and α -SMA in their stress fibers. Staining for myfibroblast markers showed that both cell types maintained their respective phenotypes when separated (Fig 2D). Importantly, no transition ($< 5\%$) of fibroblasts to myfibroblasts was observed when fibroblasts were not in contact with myfibroblasts (Fig 2E). The results show that cell-cell contact between myfibroblasts, and fibroblasts is sufficient to induce phenotype transition. Staining for myfibroblast markers showed that both cell types maintained their respective phenotypes when separated. Importantly, no transition of fibroblasts to myfibroblasts was observed when the barrier was in place. These findings indicate that cell-cell contact is necessary for the fibroblast-to-myfibroblast transition. This suggests that the mechanism driving the transition relies on direct physical interaction between the two cell types rather than solely on diffusible chemical signals, providing new insights into the process of fibroblast transition.

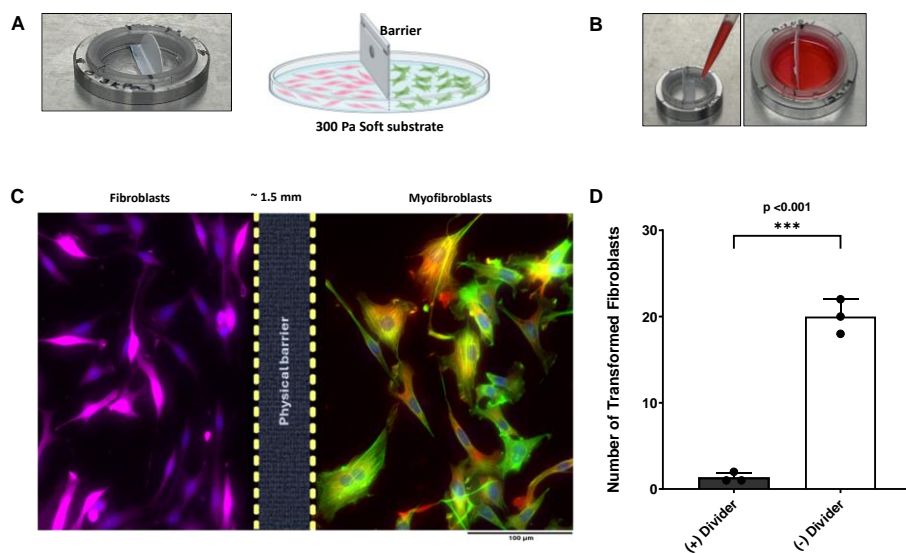


Fig 2: Cell-cell contact is necessary for the fibroblast-to-myfibroblast transitions. **(A)** A physical barrier set up on the 300Pa soft substrate separates fibroblasts from the myfibroblasts **(B)** immediate diffusion of a red dye across dish in the presence of the barrier confirmed the possibility of diffusion of any intercellular chemical signals. **(C)** Cells were stained for

myofibroblast markers, F-actin (green) and α -SMA (red) and nuclear stain DAPI (blue). Fibroblasts (magenta) did not express α -SMA in their stress fibers when not in contact with myofibroblasts despite the presence of intercellular chemical signals but myofibroblasts retained their phenotype (reddish yellow stress fibers). **(D)** Less than 5% of the fibroblasts transformed into myofibroblasts ($p < 0.001$, unpaired t-test, $n=3$).

3. Cell-cell contact triggers PLC activation

Our next objective was to elucidate the precise mechanisms occurring when cells are in contact with one another. It is well-established that signal transduction across cell membranes involves the activation of two key enzymes: phosphatidylinositol (PI)-specific phospholipase C (PLC) and phosphoinositide 3-kinase (PI 3-kinase). Typically, PLC activation occurs in response to various cellular agonists. In our study, we proposed that cells in contact utilize mechanical force as a stimulus to initiate PLC activation (Fig 3A). Specifically, we hypothesized that cell-cell contact generates force in adjacent cells, which subsequently initiates PLC activation triggering the hydrolysis of Phosphatidylinositol 4,5-bisphosphate (PI(4,5)P₂ or PIP₂). This hydrolysis results in the production of two important second messengers: inositol 1,4,5-trisphosphate (I(1,4,5)P₃ or IP₃) and diacylglycerol (DAG)^{35–37}. Therefore, to test the existence of a force-induced PLC activation mechanism in fibroblasts, we used an indenter to impose a strain field on a PDMS gel substrate, measured by displacements of beads attached to the gel. We applied a shear stress of the order of 10s of Pa, comparable to the shear stress exerted by an isolated myofibroblast³⁸, was sufficient to trigger PLC activation and PIP₂ hydrolysis in the fibroblasts. We observed a systematic decline in PIP₂ levels (measured as fluorescence intensity) in the cell ensemble, confirming PLC activation and PIP₂ hydrolysis (Fig 3B).

Given that IP₃ formation is central to two major pathways, including one initiated by G protein-linked receptors, we investigated whether fibroblast contact with myofibroblasts activated the GqGPCR pathway. We used FR900359, a cyclic depsipeptide inhibitor of G α_q , G α_{11} , and G α_{14} in a co-culture of fibroblasts and myofibroblasts on the 300Pa substrate³⁹. Cells were grown under standard culture conditions and treated with 10 μ M FR900359 for 72 hours (controls were samples that did not receive treatment). Staining for myofibroblast markers, revealed

that fibroblasts failed to transition into myofibroblasts in the presence of the GqGPCR inhibitor despite being in a co-culture setup (Fig 3D-F). Myofibroblasts remained largely unaffected under both conditions. These findings provide a valuable insight into the molecular mechanism underlying fibroblast to myofibroblast transitions, suggesting that the GqGPCR pathway is triggered upon myofibroblast contact with fibroblast and an inhibition of this pathway prevents cell-cell contact induced transition.

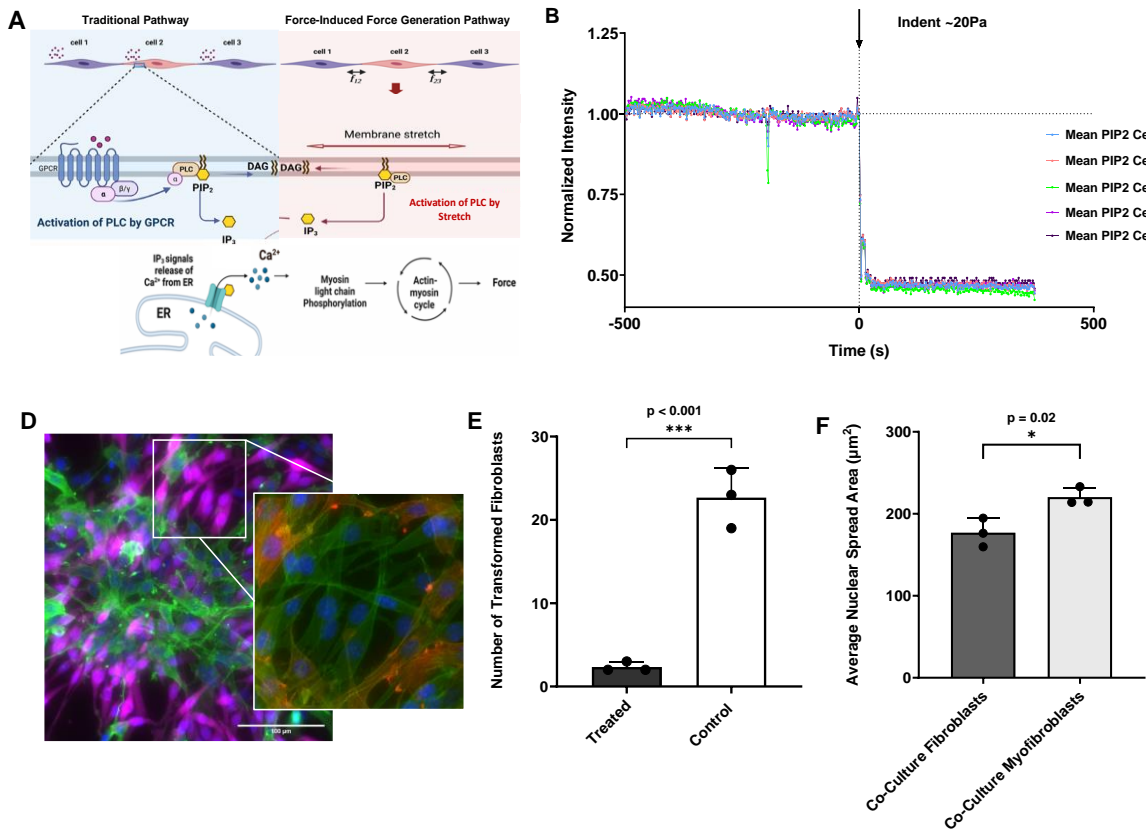


Fig 3: Cell-cell contact induces PIP₂ hydrolysis. **(A)** A force-induced force-generation mechanism in fibroblasts. **(B)** A shear stress of ~ 20 Pa was sufficient to induce PLC activation and result in PIP₂ hydrolysis, indicated by a steady decline in PIP₂ fluorescence intensity (n=1). When cells were stained for myofibroblast markers, F-actin (green) and α-SMA (red) and nuclear stain DAPI (blue) **(C)** Fibroblasts do not show α-SMA in their stress fibers, indicating that they do not transition into myofibroblasts in the presence of the GqGPCR inhibitor despite being in a co-culture for 3 days. Myofibroblasts retain α-SMA in their stress fibers (indicated by the absence of reddish yellow stress fibers). **(D)** Less than 3% fibroblasts transitioned to myofibroblasts in the presence of the inhibitor (p < 0.001, unpaired t-test, n=3). **(E)** The average nuclear spread area of

fibroblasts in the co-culture when GqGPCR pathway is inhibited, is significantly lower than that of the myofibroblasts in the same culture, indicating a lack of phenotype transition (One-way ANOVA, n=3).

The identification of this pathway as a key mediator of contact-induced force generation and cellular transformation opens new avenues for research in wound healing and fibrosis where myofibroblast activity is known to play a significant role. This finding has significant implications for understanding intercellular communication and develop potential therapeutic interventions for Idiopathic Pulmonary Fibrosis. Furthermore, this study highlights the importance of considering the physical microenvironment and cell-cell interactions in understanding cellular behavior and tissue mechanics. Future studies could explore the downstream effectors of the GqGPCR pathway in this context and investigate potential crosstalk with other mechanosensitive signaling pathways.

4. Contact between fibroblasts and myofibroblasts results in an increase of cytoskeletal tension in fibroblasts

As a next step, we investigated the potential role of mechanosensitive signaling in cell-contact-dependent transition of fibroblasts to myofibroblasts. Prior research has demonstrated that fibroblasts exhibit lower intrinsic cytoskeletal tension (cellular pre-stress) compared to myofibroblasts^{20,40}. We hypothesized that upon contact of fibroblasts with myofibroblasts, the high cytoskeletal tension in myofibroblasts may alter the cytoskeletal tension in fibroblasts, in turn triggering fibroblast-to-myofibroblast transition. In our study, we employed Monolayer Stress Microscopy (MSM) to quantify the mechanical stresses within the cells of the co-culture and calculate the net cellular contractility (Mii). MSM combines Traction Force Microscopy (TFM) with computational modeling to generate stress maps, allowing us to visualize and measure the internal mechanical tension across the cell monolayer⁴¹⁻⁴³. Briefly, the fibroblasts and myofibroblasts were co-cultured into a multicellular photopatterned ensemble. Cells were imaged after 24 hours of seeding, and we measured the traction forces exerted by cells onto a deformable 13kPa substrate embedded with fluorescent beads. By applying a mask that outlines cell-cell borders from a phase-contrast image, we reconstructed the force vectors at the cell-substrate interface. Using these

traction forces as input, MSM enabled us to compute the in-plane stresses within the monolayer, providing a detailed map of mechanical tensions between cells where we were able to separately calculate contractility due to cell-cell interactions, cell-matrix interactions, and the net contractility of each cell, as well as determine the normal and shear forces at each cell border by analyzing bead displacements⁴⁴. The underlying assumptions and limitations of this method have been detailed in previous work⁴⁵.

We observed that fibroblasts in direct contact with myofibroblasts in the co-culture ensemble exhibited increased cytoskeletal tension on day 1 (Fig 4C). This data is particularly of interest because no visible phenotypic changes are detected in the fibroblasts on day 1 co-culture with myofibroblasts on 300Pa soft substrate (Fig 4D-E). Specifically, we do not observe the expression of α -smooth muscle actin (α SMA) in stress fibers. The findings from this work are the first to suggest that an increase in cytoskeletal tension precedes phenotypic transition from fibroblasts to myofibroblasts, providing insight into the mechanical aspects of this cellular transformation.

This temporal relationship between the increase in cytoskeletal tension and the subsequent phenotypic transition suggests a causal link between these two phenomena. These findings not only shed light on the mechanical aspects of the fibroblast-to-myofibroblast transformation but also underscore the importance of cell-cell interactions and mechanical forces in regulating cellular behavior and FMT. This contributes to our understanding of the complex interplay between cellular mechanics and phenotypic plasticity in the context of tissue remodeling and fibrosis.

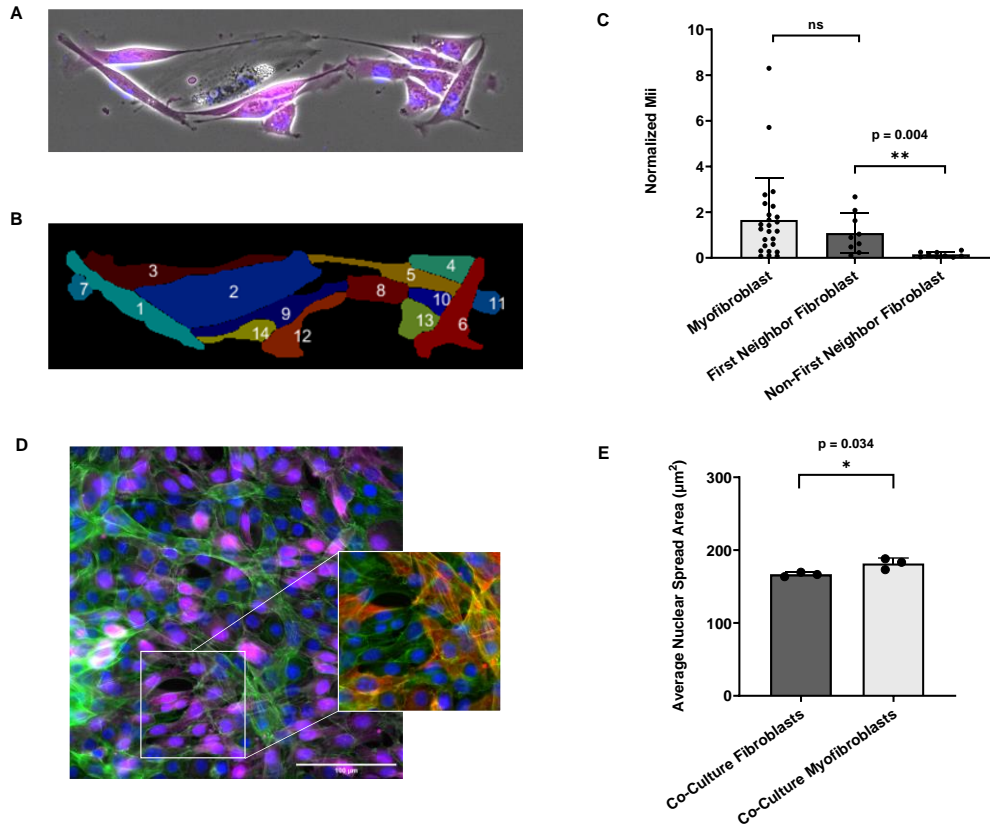


Fig 4: Fibroblasts in contact with myofibroblasts exhibit increased cytoskeletal tension on day 1. **(A-B)** representative pattern of a cellular ensemble of a myofibroblast-fibroblast culture. Nuclei are stained blue, with fibroblasts-stained (magenta). In the labeling, cell two is a myofibroblast, with 1, 3, 9 and 5 considered “first neighbors fibroblasts” as they are in direct contact with the myofibroblast, with the remaining cells considered “non-first neighbor fibroblasts” to the myofibroblast as they are not in direct contact. **(C)** Fibroblasts in contact with a myofibroblast exhibit increased contractility within 24 hours, reaching levels comparable to myofibroblasts, indicating an early mechanical transition before a documented phenotypic change (Mann-Whitney Rank Sum Test, $n=2$). In contrast, fibroblasts without direct myofibroblast contact show significantly lower contractility ($p = 0.004$, Mann-Whitney Rank Sum Test, $n=2$). **(D)** Fibroblasts do not express α -SMA in their stress fibers, indicating that they do not transition into myofibroblasts despite being contact with myofibroblasts for 24 hours (indicated by the absence of reddish yellow stress fibers). **(E)** The average nuclear spread area of fibroblasts in the co-culture, is significantly lower than that of the myofibroblasts in the same culture, indicating a lack of phenotype transition (One-way ANOVA, $n=3$)

5. Increase in cytoskeletal tension is sufficient to drive fibroblast-to-myofibroblast transition

Finally, to determine if an increase in cell prestress alone is sufficient to drive fibroblast-to-myofibroblast transition (FMT), fibroblast monocultures on the 300 Pa substrate were treated with 2.5 μ M histamine, a compound known to increase cytoskeletal prestress but not directly influence fibroblast to myofibroblast transition⁴⁶. Our observations reveal that at least 20% of the fibroblasts in the culture transitioned into myofibroblasts, suggesting that an increase in cytoskeletal prestress alone can induce fibroblast to myofibroblast transition (Fig 5A-D). These findings provide valuable insights into the mechanical regulation of phenotypic transitions and may have important implications for understanding fibrosis and wound healing processes.

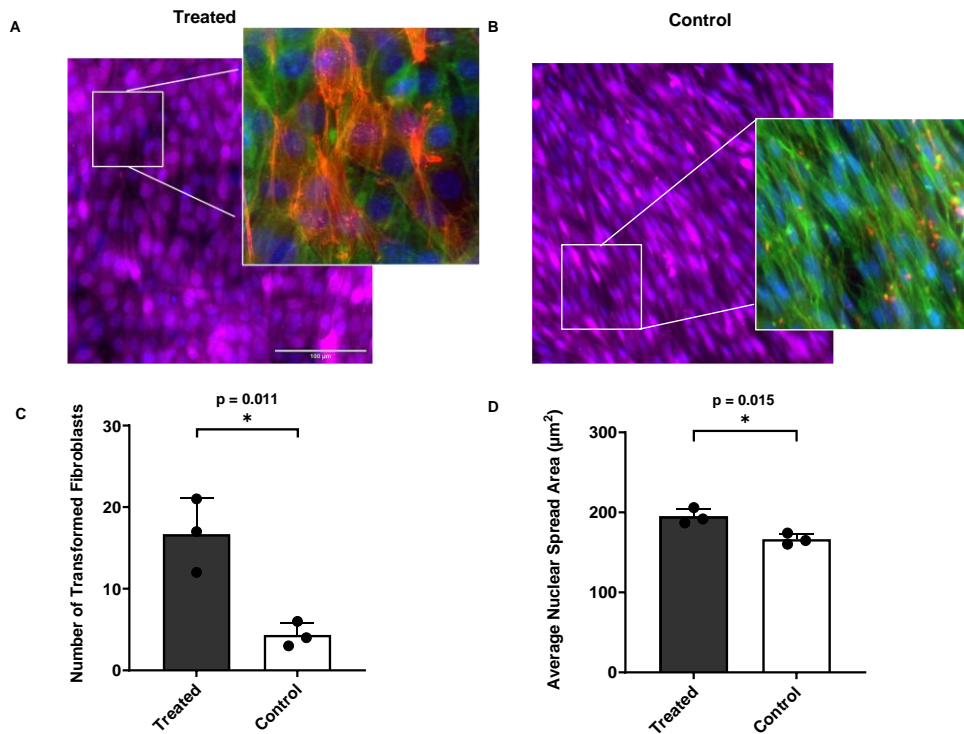


Fig 5: A rise in cytoskeletal pre-stress is sufficient to induce the transition of fibroblasts to myofibroblasts even in the absence of myofibroblast contact on a 300Pa soft substrate. **(A)** Fibroblasts (magenta) treated with 2.5 μ M histamine to increase their cytoskeletal pre-stress, show sequestration of α -SMA in their stress fibers (indicated by reddish yellow stress fibers). **(B)** Fibroblasts with no rise in cell pre-stress do not show α -SMA in their stress fibers (indicated by the absence of reddish yellow stress fibers). **(C)** Less than 5% of fibroblasts showed sequestration of α -SMA in their stress fibers in the control samples ($p =$

0.011, unpaired t-test, n=3). **(D)** The average nuclear spread area of fibroblasts treated with 2.5 μ M histamine was significantly higher ($p = 0.015$) than that of controls indicating the propensity of phenotype transition of fibroblasts with the rise in cellular pre-stress (One-way ANOVA, n=3).

Discussion

This study uncovers novel mechanisms driving fibroblast-to-myofibroblast transition (FMT) in fibrosis, challenging the traditional view that FMT is primarily governed by soluble factors or extracellular matrix (ECM) stiffness. We demonstrate that direct cell-cell contact between fibroblasts and myofibroblasts is sufficient to induce FMT, independent of biochemical or matrix-derived mechanical cues. Our findings emphasize the critical role of intercellular mechanical signaling and highlight the GqGPCR pathway as a mediator of contact-induced FMT, presenting a promising target for anti-fibrotic therapies. Furthermore, the observed increase in cytoskeletal tension preceding and driving FMT suggests that modulating cellular mechanics could be an effective therapeutic strategy.

While these results provide significant insights, limitations remain. The in vitro nature of the experiments may not fully capture the complexity of in vivo fibrotic environments. Future studies should validate these findings in 3D culture systems or animal models and further dissect the molecular mechanisms linking cell-cell contact, GqGPCR signaling, and cytoskeletal tension to FMT. Identifying key mechanotransduction players could uncover additional therapeutic targets. Further investigation into the role of specific mechanosensitive proteins and ion channels could provide additional insights into the mechanotransduction pathways involved in fibroblast-to-myofibroblast transition. Exploring the interplay between cellular mechanics and epigenetic regulation during this process may reveal novel mechanisms of fibrosis progression. Additionally, developing targeted approaches to modulate cytoskeletal tension in specific cell populations within fibrotic tissues could lead to more precise and effective therapeutic interventions.

In conclusion, this study reveals a previously unrecognized mechanism of FMT driven by direct cell-cell interactions and mechanical signaling, expanding our understanding of fibrosis progression. By highlighting the interplay between intercellular mechanical forces and cytoskeletal tension, this work opens new avenues for therapeutic interventions targeting the mechanical aspects of fibrotic disease.

Acknowledgements

The authors thank Ms. Christina Velez for providing the EFS-tdTomato lentivirus. This work was supported by the NSF Career grant #2047207 awarded to Harikrishnan Parameswaran.

Materials and Methods

1. **Fabrication of an optically clear substrate:** NuSil is an optically clear, biologically inert PDMS substrate with a tunable Young's modulus ranging from 0.3 to 70 kPa⁴⁷. To model soft healthy tissue, equal parts of NuSil gel-8100, parts A and B (NuSil, CA, USA) were mixed (1:1) to obtain a substrate with Young's modulus $E=300\text{Pa}$ and spin-coated onto 30-mm-diameter, #1.5 glass coverslips for 50 seconds to produce a 100 μm -thick layer. Similarly, a crosslinker volume 0.36% of the combined parts A and B volume was added to obtain substrates with Young's modulus $E = 13 \text{ kPa}$. Coverslips were incubated at room temperature for an hour and cured overnight at 60°C. These cured coverslips were then secured in sterile 40-mm Bioptech dishes (Biological Optical Technologies, PA, USA), UV sterilized for 1 hour, and protein coated with 0.1% gelatin solution (Millipore Sigma) for use in cell culture experiments.
2. **Fibroblast Culture:** NIH 3T3 mouse fibroblasts (Lot #70030679) acquired from ATCC were utilized for our experiments. Cells were grown under standard culture conditions of 37°C and 5% CO₂ and used by passage 20 for all experiments. Culture medium: Cells were cultured in 10% fetal bovine serum, Dulbecco's modified Eagle's medium/F12 (Fisher Scientific, Massachusetts), 1 \times penicillin/streptomycin (Fisher Scientific), 1 \times MEM nonessential amino acid solution (Sigma Aldrich, Missouri), and amphotericin B (25 $\mu\text{g/liter}$; Sigma-Aldrich).

Co-culture platform to study fibroblast-to-myofibroblast transition: Equal number of fibroblasts and myofibroblasts were plated together (or with a physical barrier to separate the cell types while allowing diffusion) on the 300Pa soft substrate. At a seeding density of 10^5 cells per cm^2 , the cells were cultured in standard cell culture medium and conditions for 72 hours in the absence of any external chemical/ mechanical cues. Cells were then analyzed for fibroblast to myofibroblast transitions.

3. **Generation of a pure fibroblast and myofibroblast population:** To visualize and distinctively identify fibroblasts, NIH 3T3-mouse fibroblasts (ATCC) were transduced with a lentiviral vector encoding tandem-dimer Tomato fluorescence protein (tdTomato, Vector Builder, catalog no. VB181014-1005thm). Briefly, the cells were seeded and cultured according to standard cell culture protocol and after 18 hours, cells were introduced to cell culture medium containing polybrene (5 $\mu\text{g}/\text{ml}$; Thermo Fisher Scientific, catalog no. TR1003G) and the manufacturer's recommended functional titer concentration of lentiviruses. After 24 hours of exposure to the transduction medium, cells were allowed to recover in unadulterated cell culture medium for an additional 24 to 48 hours. Next, cell selection was performed by adding culture medium containing blasticidin (8 $\mu\text{g}/\text{ml}$; Sigma-Aldrich, catalog no. 15205). This pure 3T3-mouse fibroblast population expressing tdTomato (3T3-tdT) was expanded on protein coated 300Pa soft substrates and cultured for up to at least 6 additional passages before being used in experiments, or they were continued to be expanded on the soft substrate for use within 20 passages since the time of thawing the cells. Cells were harvested using Gibco TrypLE Select reagent. To generate a myofibroblast population, non-transduced 3T3-mouse fibroblasts were cultured for a period of at least 4 weeks on tissue culture plastic ($\geq 100\text{kPa}$) and utilized within passage 20 for all experiments. Myofibroblasts were identified as cells that stained positive for α -SMA in stress fibers[3].
4. **Immunostaining and microscopy:** Cells were fluorescently labeled for filamentous actin (F-actin) and alpha smooth muscle actin (α -SMA). Cells were fixed in 4% paraformaldehyde in PBS at room temperature for 10 min. Then, cells were permeabilized with 100% ethanol for 10 min at 20°C . Following permeabilization, cells were blocked using $1\times$ PBS containing 0.1% Tween 20, 1% bovine serum albumin (BSA), and glycine (22.52

mg/ml) for 30 min at room temperature. Next, cells were labelled with Alpha-Smooth Muscle Actin Monoclonal Antibody (1A4), eFluor™ 660, eBioscience™ (Cat #50-9760-82) at 5 µg/mL in 1× PBS containing 1% BSA and simultaneously stained for Filamentous actin with ActinGreen™ 488 ReadyProbes™ Reagent (AlexaFluor™ 488 phalloidin, Cat# R37110) for 1 hour at room temperature. Cells were washed 3 times with 1X PBS to remove non-specific binding. Lastly, cell nuclei were labeled with NucBlue (Fisher Scientific, Waltham, MA, USA) and mounted using ProLong™ Glass Antifade Mountant (Cat #P36984). Images were acquired with a Leica DMI8 inverted microscope, a Leica DFC6000 camera, and a Leica LED8 light engine (excitation, 480/40 nm; emission, 527/50 nm) using a 40x/0.65 dry objective (Leica DMI8 microscope, Leica, Wetzlar, Germany).

5. **Applying a point displacement on the matrix:** We fixed a nail dotting tool (ORLY, California) with a 1.5 mm diameter ball-end to the InjectMan 4 micromanipulator (Eppendorf, Germany) on our Leica DMI8 microscope. The micromanipulator allowed precise control of this tool with which we applied a transient poke to the extracellular matrix some distance away (~300µm) from adhered cells at a 45° angle and depth of 30µm to generate a shear stress of the order of 10s of Pa, comparable to that of a myofibroblast.
6. **Fluorescent PIP2 Imaging:** Fibroblasts were loaded with a fluorescent cytosolic PIP2 indicator to record changes in [PIP2] using a live green downward phosphatidylinositol 4,5-biphosphate (PIP2) assay kit (#D0400G), Montana Molecular (Montana). The assay genetically encodes fluorescent protein expression using a BacMam vector. Following the protocol provided, we transduced cultured fibroblasts with the PIP2 sensor for 24 hours at 37°C and 5% CO₂. Prior to imaging, cells were washed with Hanks' Balanced Salt Solution (HBSS) and incubated at 37°C and 5% CO₂ in for an additional 30 minutes. The cells were washed once more before imaging. 16-bit images were recorded at 0.5 Hz for 5 minutes before indentation (~20Pa) and at least 5 minutes post indentation. Cells were imaged with a Leica DMI8 inverted microscope, a Leica DFC6000 camera, and a Leica LED8 light engine (excitation, 480/40 nm; emission, 527/50 nm) with a 40x/0.65 dry objective. The excitation and emission wavelengths for the PIP2 was ex:480 nm/ em:515 nm. To analyze data,

each image sequence was loaded in Fiji ImageJ, and regions of interest (ROIs) were hand-selected in the cytoplasm of each cell to obtain mean grayscale intensities over the area of the ROI for each frame in time. Obtained intensities were normalized with the baseline average to plot normalized intensity values using GraphPad Prism ver. 10.4.1.

7. **Patterning cell ensembles:** We utilized the Alvéole's PRIMO optical module and the Leonardo software, a UV-based, contactless photopatterning system (Alvéole, Paris, France). 13kPa NuSil substrates coated with a layer of fluorescent beads as fiducial markers for traction force microscopy were utilized. A 5% solution of 0.2- μm -diameter green, fluorescent carboxylate-modified microspheres (FluoSpheres, Invitrogen, Carlsbad, CA, USA) in PBS was vortexed for 10 seconds. Solution (2 ml) was added to each substrate in a Biotech dish and left at room temperature for 1 hour to allow the beads to adhere. The bead solution was poured off, substrates were washed three times with PBS, and then PBS was poured off. Substrates were then protein coated with 0.1% gelatin solution for use in cell culture. The substrate surface was first coated with 500 $\mu\text{g}/\text{mL}$ PLL (Sigma Aldrich, St. Louis, MO, USA) for 1 hour at room temperature. The substrate was washed with PBS and 10 mM HEPES buffer adjusted to pH 8.0 and incubated with 50 mg/mL mPEG-SVA (Laysan Bio, Inc., Arab, AL, USA) at room temperature for 1 hour, and washed with PBS once more. The PRIMO system was calibrated using fluorescent highlighter on an identical substrate. The PBS was replaced by 14.5 mg/mL PLPP (Alvéole, Paris, France), and then the desired pattern, previously created with graphic software, was illuminated with UV light focused on the substrate surface for 30 seconds. Patterned surfaces were washed again with PBS and then incubated with 0.1% gelatin for 1 hour at room temperature. The substrate was washed and hydrated in standard cell culture media. Fibroblasts and myofibroblasts were added to the patterned surfaces at a cell density of 3×10^4 cells/ml to obtain a confluent pattern of the two cell types within 24 hours.
8. **Traction Force Microscopy and Monolayer Stress Microscopy measurements:** Traction force measurements were recorded by imaging the fluorescent beads with a 20x/0.55 dry objective and the Leica DMI8 microscope. Images were taken at baseline, during the experiment, and after cells were removed (using RLT Lysis Buffer, Qiagen, Hilden,

Germany). Using these images, cellular forces were calculated with a custom MATLAB (MathWorks, Natick, MA, USA) software program using Fourier Traction Force Microscopy (TFM). To calculate the net contractility of each cell within a multicellular ensemble, we employed monolayer stress microscopy (MSM). This computational approach estimates stresses in a cell layer based on the forces at the cell-matrix interface. Initially, traction force vectors obtained from traction force microscopy (TFM) were processed using a modified version of the open-source Python code, pyTFM. By applying a mask that outlines cell-cell borders from a phase-contrast image, we were able to separately calculate contractility due to cell-cell interactions, cell-matrix interactions, and the net contractility of each cell, as well as determine the normal and shear forces at each cell border.

9. **Measurement of nuclear spread area:** The nuclear spread area represented in this manuscript is the average nuclear area of 10 cells in each dish (n). 40X images were loaded into Fiji ImageJ, and regions of interest (ROIs) were hand-selected in the DAPI images using the ellipse tool, by tracing the outline of the nucleus. The area of selection is in square pixels and represented as μm^2 as it was spatially calibrated using the Analyze>Set Scale option.
10. **Data presentation and statistical testing:** Throughout the manuscript, we represent data as the average of N independent trials. The error bars indicate SD over independent trials. The individual data points are shown in all bar plots. SigmaPlot ver.11 build 11.0.0.75 (Systat Software, San Jose, CA) was used to perform statistical tests. One-way ANOVAs followed by post-hoc pairwise comparisons were used to test for significant differences in datasets of three or more groups, which were influenced by one independent factor. Pairwise comparisons were performed using the t-test when data were normally distributed. Otherwise, the Mann-Whitney rank-sum test was used to compare median values. The specific tests used, number of samples, and P value are described along with the corresponding results.

References

1. Spagnolo, P. *et al.* Idiopathic pulmonary fibrosis: Disease mechanisms and drug development. *Pharmacol Ther* **222**, 107798 (2021).
2. Martinez, F. J. *et al.* Idiopathic pulmonary fibrosis. *Nat Rev Dis Primers* **3**, 17074 (2017).
3. Raghu, G., Weycker, D., Edelsberg, J., Bradford, W. Z. & Oster, G. Incidence and Prevalence of Idiopathic Pulmonary Fibrosis. *Am J Respir Crit Care Med* **174**, 810–816 (2006).
4. Johansson, K. A. *et al.* Acute exacerbation of idiopathic pulmonary fibrosis associated with air pollution exposure. *European Respiratory Journal* **43**, 1124–1131 (2014).
5. Hinz, B. Formation and Function of the Myofibroblast during Tissue Repair. *Journal of Investigative Dermatology* **127**, 526–537 (2007).
6. Darby, I., Skalli, O. & Gabbiani, G. Alpha-smooth muscle actin is transiently expressed by myofibroblasts during experimental wound healing. *Lab Invest* **63**, 21–9 (1990).
7. Desmouliere, A., Darby, I. A., Laverdet, B. & Bonté, F. Fibroblasts and myofibroblasts in wound healing. *Clin Cosmet Investig Dermatol* 301 (2014) doi:10.2147/CCID.S50046.
8. Serini, G. & Gabbiani, G. Mechanisms of Myofibroblast Activity and Phenotypic Modulation. *Exp Cell Res* **250**, 273–283 (1999).
9. Hinz, B., Celetta, G., Tomasek, J. J., Gabbiani, G. & Chaponnier, C. Alpha-Smooth Muscle Actin Expression Upregulates Fibroblast Contractile Activity. *Mol Biol Cell* **12**, 2730–2741 (2001).
10. Wang, J., Zohar, R. & McCulloch, C. A. Multiple roles of α -smooth muscle actin in mechanotransduction. *Exp Cell Res* **312**, 205–214 (2006).
11. Hinz, B., Celetta, G., Tomasek, J. J., Gabbiani, G. & Chaponnier, C. *Alpha-Smooth Muscle Actin Expression Upregulates Fibroblast Contractile Activity. Molecular Biology of the Cell* vol. 12 (2001).
12. Hinz, B., Dugina, V., Ballestrem, C., Wehrle-Haller, B. & Chaponnier, C. A-Smooth Muscle Actin Is Crucial for Focal Adhesion Maturation in Myofibroblasts. *Molecular Biology of the Cell* vol. 14 2508–2519 Preprint at <https://doi.org/10.1091/mbc.E02-11-0729> (2003).
13. Hinz, B. The role of myofibroblasts in wound healing. *Curr Res Transl Med* **64**, 171–177 (2016).

14. Ju, X. *et al.* Regulation of myofibroblast dedifferentiation in pulmonary fibrosis. *Respir Res* **25**, 284 (2024).
15. Moore, M. W. & Herzog, E. L. Regulation and Relevance of Myofibroblast Responses in Idiopathic Pulmonary Fibrosis. *Curr Pathobiol Rep* **1**, 199–208 (2013).
16. Plantier, L. *et al.* Physiology of the lung in idiopathic pulmonary fibrosis. *European Respiratory Review* **27**, 170062 (2018).
17. Plikus, M. V. *et al.* Fibroblasts: Origins, definitions, and functions in health and disease. *Cell* **184**, 3852–3872 (2021).
18. Noble, P. W. *et al.* Pirfenidone in patients with idiopathic pulmonary fibrosis (CAPACITY): two randomised trials. *Lancet* **377**, 1760–9 (2011).
19. Wollin, L. *et al.* Mode of action of nintedanib in the treatment of idiopathic pulmonary fibrosis. *Eur Respir J* **45**, 1434–45 (2015).
20. Tomasek, J. J., Gabbiani, G., Hinz, B., Chaponnier, C. & Brown, R. A. Myofibroblasts and mechano: Regulation of connective tissue remodelling. *Nature Reviews Molecular Cell Biology* vol. 3 349–363 Preprint at <https://doi.org/10.1038/nrm809> (2002).
21. Tschumperlin, D. J., Ligresti, G., Hilscher, M. B. & Shah, V. H. Mechanosensing and fibrosis. *J Clin Invest* **128**, 74–84 (2018).
22. Freeberg, M. A. T. *et al.* Mechanical Feed-Forward Loops Contribute to Idiopathic Pulmonary Fibrosis. *Am J Pathol* **191**, 18–25 (2021).
23. Staab-Weijnitz, C. A. Fighting the Fiber: Targeting Collagen in Lung Fibrosis. *Am J Respir Cell Mol Biol* **66**, 363–381 (2022).
24. Craig, V. J., Zhang, L., Hagood, J. S. & Owen, C. A. Matrix metalloproteinases as therapeutic targets for idiopathic pulmonary fibrosis. *Am J Respir Cell Mol Biol* **53**, 585–600 (2015).
25. Henry, M. T. *et al.* Matrix metalloproteinases and tissue inhibitor of metalloproteinase-1 in sarcoidosis and IPF. *Eur Respir J* **20**, 1220–7 (2002).
26. Bouros, D. & Antoniou, K. M. Current and future therapeutic approaches in idiopathic pulmonary fibrosis. *European Respiratory Journal* **26**, 693–703 (2005).
27. Bonella, F., Spagnolo, P. & Ryerson, C. Current and Future Treatment Landscape for Idiopathic Pulmonary Fibrosis. *Drugs* **83**, 1581–1593 (2023).

28. Arshad, M., Athar, Z. M. & Hiba, T. Current and Novel Treatment Modalities of Idiopathic Pulmonary Fibrosis. *Cureus* **16**, e56140 (2024).
29. Cilli, A. & Uzer, F. Disease progression in idiopathic pulmonary fibrosis under anti-fibrotic treatment. *Sarcoidosis Vasc Diffuse Lung Dis* **40**, e2023034 (2023).
30. Mei, Q., Liu, Z., Zuo, H., Yang, Z. & Qu, J. Idiopathic Pulmonary Fibrosis: An Update on Pathogenesis. *Front Pharmacol* **12**, (2022).
31. Shenderov, K., Collins, S. L., Powell, J. D. & Horton, M. R. Immune dysregulation as a driver of idiopathic pulmonary fibrosis. *J Clin Invest* **131**, (2021).
32. Balestrini, J. L., Chaudhry, S., Sarrazy, V., Koehler, A. & Hinz, B. The mechanical memory of lung myofibroblasts. *Integrative Biology* **4**, 410–421 (2012).
33. Kirk, T., Ahmed, A. & Rognoni, E. Fibroblast Memory in Development, Homeostasis and Disease. *Cells* **10**, 2840 (2021).
34. Hillsley, A. *et al.* A strategy to quantify myofibroblast activation on a continuous spectrum. *Sci Rep* **12**, 12239 (2022).
35. Bae, Y. S. *et al.* Activation of Phospholipase C- γ by Phosphatidylinositol 3,4,5-Trisphosphate. *Journal of Biological Chemistry* **273**, 4465–4469 (1998).
36. Berridge, M. J. Inositol trisphosphate and calcium signalling. *Nature* **361**, 315–325 (1993).
37. Rhee, S. G. & Bae, Y. S. Regulation of Phosphoinositide-specific Phospholipase C Isozymes. *Journal of Biological Chemistry* **272**, 15045–15048 (1997).
38. Munevar, S., Wang, Y. & Dembo, M. Regulation of mechanical interactions between fibroblasts and the substratum by stretch-activated Ca²⁺ entry. *J Cell Sci* **117**, 85–92 (2004).
39. Schrage, R. *et al.* The experimental power of FR900359 to study Gq-regulated biological processes. *Nat Commun* **6**, 10156 (2015).
40. Li, B. & Wang, J. H.-C. Fibroblasts and myofibroblasts in wound healing: force generation and measurement. *J Tissue Viability* **20**, 108–20 (2011).
41. Tambe, D. T. *et al.* Collective cell guidance by cooperative intercellular forces. *Nat Mater* **10**, 469–475 (2011).
42. Patel, N. G. *et al.* Unleashing shear: Role of intercellular traction and cellular moments in collective cell migration. *Biochem Biophys Res Commun* **522**, 279–285 (2020).

43. Ng, M. R., Besser, A., Brugge, J. S. & Danuser, G. Mapping the dynamics of force transduction at cell–cell junctions of epithelial clusters. *Elife* **3**, (2014).
44. Bauer, A. *et al.* pyTFM: A tool for traction force and monolayer stress microscopy. *PLoS Comput Biol* **17**, e1008364 (2021).
45. Tambe, D. T. *et al.* Monolayer Stress Microscopy: Limitations, Artifacts, and Accuracy of Recovered Intercellular Stresses. *PLoS One* **8**, e55172 (2013).
46. Gailit, J., Marchese, M. J., Kew, R. R. & Gruber, B. L. The differentiation and function of myofibroblasts is regulated by mast cell mediators. *J Invest Dermatol* **117**, 1113–9 (2001).
47. Yoshie, H. *et al.* Traction Force Screening Enabled by Compliant PDMS Elastomers. *Biophys J* **114**, 2194–2199 (2018).